

Cite this: *RSC Adv.*, 2014, 4, 43029

Synthesis and evaluation of macroporous polymerized solid acid derived from Pickering HIPEs for catalyzing cellulose into 5-hydroxymethylfurfural in an ionic liquid

Heping Gao,^a Yinxian Peng,^{*a} Jianming Pan,^{*b} Jun Zeng,^a Changhua Song,^b Yunlei Zhang,^b Yongsheng Yan^b and Weidong Shi^b

Stable water-in-oil (W/O) Pickering high internal phase emulsions (HIPEs) with an internal phase volume fraction of 84.8% were first stabilized by both the hydrophobic silica nanoparticles and span 80. Then, based on the obtained Pickering HIPEs, several macroporous polymerized solid acid (PDVB-SS-X-SO₃H, X = 0, 0.2, 0.6) were prepared by polymerizing divinyl benzene (DVB) and sodium *p*-styrenesulfonate (SS), and were subsequently combined with sulfonation in H₂SO₄. All the as-prepared PDVB-SS-X-SO₃H possessed open-cell structure, interconnecting pores and strong acidity, and were adopted as catalysts to convert cellulose into 5-hydroxymethylfurfural (HMF) in the presence of [Emim]Cl-mediated solvents. The results showed a maximum yield of 29.6% for PDVB-SS-0.2-SO₃H, 12.9% for PDVB-SS-0-SO₃H and 15.5% for PDVB-SS-0.6-SO₃H under the same condition within 2.0 h at 120 °C, suggesting that the pore sizes and strong acidic sites played a key role in cellulose conversion. PDVB-SS-X-SO₃H can be very easily recycled at least four times without a significant loss of activity. This research opens up a new method to synthesize porous solid acid catalyst materials through Pickering HIPEs templates.

Received 9th July 2014
Accepted 26th August 2014

DOI: 10.1039/c4ra06870j

www.rsc.org/advances

1 Introduction

With the decrease in fossil fuel reserves, cellulose, an abundant and renewable resource, is attracting increasing attention as a replacement for fossil fuels.¹ For using cellulose to produce fuel, producing 5-hydroxymethylfurfural (HMF) from cellulose in one step is a very important process.² In the literature, it has been shown that HMF can be simply converted into furan bio-fuels, which can replace fossil fuels and chemicals by condensation and hydrogenolysis reactions. For example, HMF can be hydrogenolysed into 2,5-dimethylfuran (2,5-DMF), which is a potential fuel³ having higher energy density than ethanol. In addition, 2,5-bis(hydroxymethyl)furan (2,5-BHF) and 2,5-diformylfuran (2,5-DFF), which are widely used in the synthesis of polymers, can also be produced from HMF.⁴ In recent years, the catalytic conversion of cellulose into HMF has been investigated by various acid catalysts. Homogeneous acid catalysts, such as HCl⁵ and organic acids,⁶ have been used and high yields of HMF have been obtained from the degradation of cellulose. However, the disadvantages of the difficult separation of the catalyst from the liquid reaction medium, environmental unfriendliness,

corrosive nature and high corrosion of equipment has limited the further application of homogeneous acid catalysts in industry. With the enhancement in environmental protection awareness, heterogeneous acid catalysts are increasingly being used in the degradation of cellulose to HMF, due to their environmentally friendly nature, better recyclability, green chemical processes, ease of separation of the catalyst from the solution system, and reduced corrosion to equipment. Moreover, in recent years, solid acid catalysts, such as solid immobilized liquid acid, zeolites,⁷ sulfide,⁸ natural clay minerals,⁹ ion-exchanged resins,¹⁰ heteropoly acids (HPA),¹¹ oxides,¹² metal salts,¹³ sulfonated carbon-based solid acid¹⁴ and polymer-based solid acid,¹⁵ are being widely used in various acid-catalyzed reactions.

Recently, more and more researchers have found that porous solid acids have extraordinary catalytic activities due to excellent thermal stability, adjustable pore, high specific surface area, lower density, high catalytic activity and environmentally friendliness. For example, Fujian Liu *et al.*¹⁶ successfully prepared porous polydivinylbenzene (PDVB) based solid strong acid (PDVB-SO₃H-SO₂CF₃) by grafting the strong electron withdrawing group of SO₂CF₃ onto the network of preformed porous solid acid of PDVB-SO₃H, which could be synthesized by the sulfonation of superhydrophobic porous PDVB or the copolymerization of DVB with sodium *p*-styrene sulfonate. Caio Tagusagawa *et al.*¹⁷ prepared several porous Ta-W mixed oxide

^aSchool of biology and Chemical Engineering, Jiangsu University of science and technology, Zhenjiang 212013, China

^bSchool of Chemistry and Chemical Engineering, Jiangsu University, Zhenjiang 212013, China. E-mail: zhenjiangpjm@126.com

solid acids from TaCl_5 and WCl_6 in the presence of poly block copolymer surfactant pluronic P-123. Although the catalytic application effect was obvious, the catalysts were prepared in harsh reaction conditions and it was hard to control the morphology of the product. To overcome these problems, our groups^{18,19} have worked on two aspects. On one hand, two acid-chromic chloride bi-functionalized catalysts, *i.e.* $\text{ATP-SO}_3\text{H-Cr(III)}$ and $\text{HNTs-SO}_3\text{H-Cr(III)}$, were successfully synthesized by grafting the $-\text{SO}_3\text{H}$ and Cr(III) onto the surface of treated attapulgite (ATP) and halloysite nanotubes (HNTs), respectively. On the other hand, based on HNTs by precipitation polymerization and Pickering emulsion polymerization, two polymeric solid acid catalysts, *i.e.* $\text{HNTs-polystyrene (PSt) - polydivinylbenzene (PDVB)-SO}_3\text{H(I)}$ and $\text{HNTs-PSt-PDVB-SO}_3\text{H(II)}$, were successfully prepared after sulfonation by 98% H_2SO_4 . Therefore, the emulsion templates method²⁰ was found to be easier and more convenient for synthesizing the porous solid acid material.

The high internal phase emulsions (HIPEs) with the controlled volume fraction of droplet higher than 74% were adopted to synthesize porous solid acid catalyst materials and subsequent polymerization of the continuous phase, commonly known as polyHIPEs.²¹ Moreover, the porous structure is adjustable by changing the volume ratio of the oil and water phase. However, the traditional polyHIPEs synthesized from surfactants, such as span 80, with between 5 and 50% (ref. 22) stabilized water-in-oil (W/O) HIPEs have poor mechanical properties.²³ However, the poor mechanical properties of polyHIPEs can be improved by increasing the continuous organic phase volume using particle reinforcements or by changing the composition of the monomer.²⁴ Among them, increasing small amounts of non-ionic polymeric surfactant to W/O particle-stabilized HIPE templates (Pickering-HIPEs) can lead to the formation of poly-Pickering-HIPEs with an open porous structure and good mechanical properties.²⁵ To the best of our knowledge, the use of Pickering HIPEs to produce the porous polymer solid acid catalyst is rarely reported.

Inspired by the discussion above, $\text{PDVB-SS-X-SO}_3\text{H}$ (X is the volume of span 80 and $X = 0, 0.2, 0.6$) with open-cell structure, interconnecting pores and strong acidity were designed and synthesized by applying to Pickering HIPEs template method. First, in the Stöber's method, modified hydrophobic silica particles²⁶ and span 80 were both used to stabilize W/O Pickering HIPEs with 84.8% in the internal phase. The internal (water) phase contained K_2SO_4 and sodium *p*-styrene sulfonate (SS) and the external (oil) phase consisted of divinylbenzene (DVB) and α,α' -azoisobutyronitrile (AIBN), which were emulsified to form stable W/O Pickering HIPEs. Then, poly-Pickering-HIPEs were sulfonated by 98% H_2SO_4 to introduce the group of $-\text{SO}_3\text{H}$ and $\text{PDVB-SS-X-SO}_3\text{H}$ was obtained. The morphology and various properties of $\text{PDVB-SS-X-SO}_3\text{H}$ were characterized and its catalytic activity was studied in detail by optimizing the reaction time, temperature and catalysts loading amounts in catalyzing cellulose to HMF (Scheme 1). It could be seen that $\text{PDVB-SS-X-SO}_3\text{H}$ showed good recyclability and chemical stability.

2 Experimental

2.1 Chemical and reagents

All the reagents were of analytical grade and were used without further purification. Tetraethoxysilane (TEOS), DVB, formic acid, levulinic acid, 5-HMF (>99%), 1-ethyl-3-methylimidazolium chloride ([Emim]Cl, >99%), azobisisobutyronitrile (AIBN), 3-methacryloxypropyltrimethoxysilane (KH-570), cellulose, toluene, ethanol, methanol, span 80, K_2SO_4 , potassium persulfate (KPS), $\text{NH}_3 \cdot \text{H}_2\text{O}$ (25 wt%), sodium *p*-styrene sulfonate (SS), and acetone were purchased from Aladdin reagent CO., LTD (Shanghai, China).

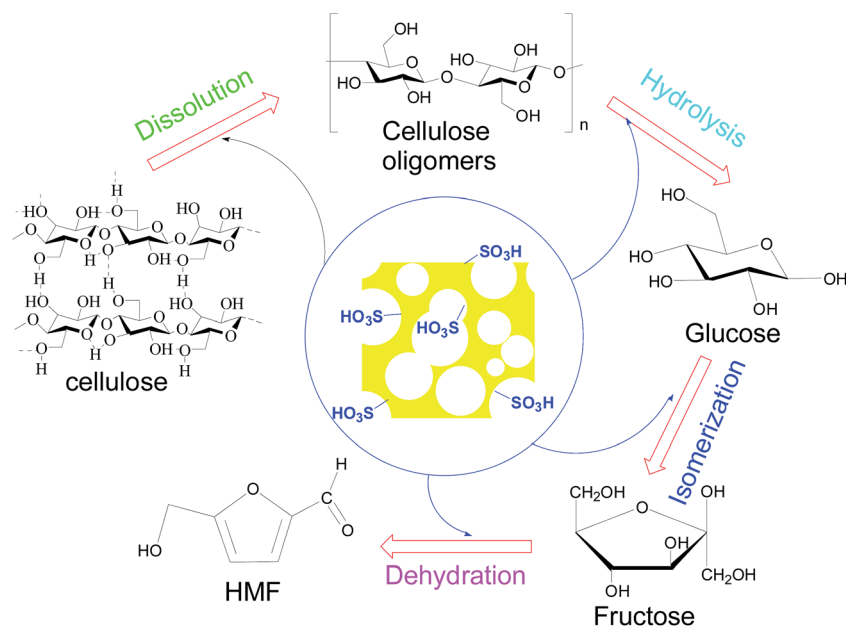
2.2 Instruments

Infrared spectra ($4000\text{--}400\text{ cm}^{-1}$) were recorded on a Nicolet NEXUS-470 FTIR apparatus (U.S.A.). The morphology of $\text{PDVB-SS-X-SO}_3\text{H}$ was observed by field emission scanning electron microscopy (SEM, JSM-7100F). The image of the silica particles was obtained by transmission electron microscopy (TEM, JEM-2100). The optical micrographs of Pickering HIPEs were collected by a DMM-330C optical microscope equipped with a high performance digital camera (CAIKON, China). X-ray photoelectron spectroscopy (XPS) of $\text{PDVB-SS-X-SO}_3\text{H}$ was recorded by the Vario EL III elemental analyzer (Elementar, Hanau, Germany). The acidity of $\text{PDVB-SS-X-SO}_3\text{H}$ was measured by NH_3 temperature-programmed desorption (NH_3 -TPD, finesorb3010) instrument. The water contact angle of silica nanoparticles were measured through the optical contact angle measuring device (KSV CM200). The detailed test procedure is described as follows. First, silica nanoparticles sample plates were prepared by spreading a thin layer of silica nanoparticles with double-sided adhesive tape on the glass. Then, 2.0 μL of deionized water was injected on the sample surface through the syringe pump and the images of the water droplet were obtained using the camera in measuring device after the water droplet was formed on the sample surface (30s). Finally, these images were analyzed using the supplied software to determine the contact angle of the sample.

2.3 Synthesis and hydrophobic modification of silica nanoparticles

Synthesis of silica nanoparticles by hydrolysis and condensation reaction was carried out according to previous literature with a slight modification.²⁶ In a typical run, 6.0 mL of TEOS was added into a solution containing 90 mL alcohol and 10 mL H_2O . Then, 3.14 mL of $\text{NH}_3 \cdot \text{H}_2\text{O}$ (25 wt%) was slowly injected into the mixture at 30°C , and the reaction was allowed to proceed for 1.0 h under mechanical stirring. Next, the reaction products were washed with alcohol several times by centrifugation, and subsequently dried at 80°C for 3.0 h in a drying oven. Finally, the uniformly sized silica nanoparticles were obtained.

The silica nanoparticles were further modified to attain hydrophobicity. A typical procedure used is detailed as follows: first, a mixture of silica nanoparticles (1.0 g), toluene (150 mL), H_2O (15 mL), and KH-570 (3.5 mL) was stirred for 24 h at 40°C . Then, the reaction products were washed with alcohol several



Scheme 1 PDVB-SS-X-SO₃H catalyzed conversion of cellulose into HMF in [Emim]Cl under atmospheric pressure.

times by centrifugation, and dried at 80 °C for 3.0 h in a drying oven. Finally, hydrophobic silica nanoparticles were obtained.

2.4 Synthesis of PDVB-SS-X-SO₃H

For the fabrication of stable W/O Pickering HIPEs, the recipes of the aqueous phase and the organic phase used are listed in Table 1. Two phases were mixed to achieve homogeneous W/O Pickering HIPEs. First, the aqueous phase was added drop by drop to the organic phase with fast and continuous stirring. Second, the HIPEs were transferred into a plastic centrifuge tube and polymerized in a circulating air oven at 60 °C for 12 h. Then, the obtained poly-Pickering-HIPEs were dried at 30 °C for 24 h in a vacuum oven until a constant weight was achieved. Small molecules in poly-Pickering-HIPEs were removed by Soxhlet extraction in deionized water at 80 °C for 24 h, and then in acetone for an additional at 80 °C for 24 h. Finally, the poly-Pickering-HIPEs, named as PDVB-SS-X (*X* standing for the volume of span 80 and *X* = 0, 0.2, 0.6) were dried at 80 °C for 12 h.

For the preparation of sulfonated solid acid catalysts, PDVB-SS-X were sulfonated by aromatic substitutions in 98% H₂SO₄.

In a typical run, the mixtures of 1.0 g of PDVB-SS-X particle and 30 mL of 98% H₂SO₄ were continuously stirred at 70 °C for 12 h. The reaction products were filtered, repeatedly washed with deionized water to remove the excess H₂SO₄, and then dried in vacuum at 80 °C for 3.0 h. Finally, the PDVB-SS-X-SO₃H were obtained.

2.5 Conversion of cellulose to HMF

The conversion of cellulose to HMF was carried out as described in previous literature with a slight modification.²⁷ In a typical run, the pretreatment of degraded cellulose was performed by adding 0.1 g of D-cellulose powder and 2.0 g of [Emim]Cl into a 15 mL of round-bottom flask and stirring the mixture at 120 °C for 30 min, which resulted in the breaking of the hydrogen bonds of cellulose molecules, and the reduction of the degree of crystallization and the regularity of the cellulose molecules. Then, the 40 mg of sulfonated PDVB-SS-X-SO₃H was added into the mixed solution, and the cellulosic reaction was further carried out at 120 °C for 2.0 h. Finally, the reaction products were diluted 5000 times in deionized water, and the concentration of HMF was analyzed by a 1200 Agilent high

Table 1 Recipes of HIPEs

Sample ^a	External, organic phase				Internal, aqueous phase			
	DVB (mL)	AIBN (g)	Silica (g)	Span 80 (mL)	Water (g)	K ₂ SO ₄ (g)	KPS (g)	SS (g)
PDVB-SS-0-SO ₃ H	3.0	0.04	1.0	0	16.8	0.08	0.04	0.2
PDVB-SS-0.2-SO ₃ H	3.0	0.04	0.3	0.2	16.8	0.08	0.04	0.2
PDVB-SS-0.6-SO ₃ H	3.0	0.04	0.3	0.6	16.8	0.08	0.04	0.2

^a PDVB-SS-X-SO₃H, *X* stand for the volume of span 80.

performance liquid chromatography (HPLC) equipped with an Agilent TC-C18 Column (4.6 × 250 mm, 5.0 mm) and a UV detector. During the analysis procedure, 20 µL of HMF samples were injected manually, separated through the Agilent TC-C18 column and detected by a UV-vis spectrophotometer at 283 nm. The column temperature was set at 25 °C and the flow rate of optimized mobile phase consisting of water and methanol with a volume ratio of 30 : 70 was set at 0.7 mL min⁻¹. Then, based on the standard curve obtained with standard substances, the concentration of HMF was obtained, and the HMF yield (*Y*, mol%) was calculated using the following equation:

$$Y\% = \frac{n_1}{n_0} \times 100\%$$

where *n*₁ (mol) and *n*₀ (mol) are the moles of HMF and the moles of glucose units of initial cellulose, respectively.

3 Results and discussion

3.1 Fabrication of hydrophobic silica nanoparticles

The morphologies of silica nanoparticles and modified silica nanoparticles were observed by TEM. As shown in Fig. 1a and b, silica nanoparticles and hydrophobic silica nanoparticle samples exhibited a sphere-shaped morphology with similar particle sizes (around 100 ± 20 nm). It was clearly seen that the surfaces of silica nanoparticles were smooth. However, the surface of the hydrophobic silica nanoparticles had a pale shadow on their rough surface, and some of those were linked together, suggesting that the vinyl groups may be grafted on the surface of silica nanoparticles. The image of the water contact angle of silica nanoparticles and hydrophobic silica

nanoparticles are shown in Fig. 1c and d. The values of silica nanoparticles of 34.7° and hydrophobic silica nanoparticles of 123.2° further illustrated the success of modification with vinyl groups. Moreover, the hydrophobic silica nanoparticles properly stabilized W/O HIPEs, which was confirmed by Binks's work regarding using the particles with the water contact angle of 123° to stabilize W/O HIPEs.²⁸

3.2 Formation of Pickering W/O HIPEs

In this work, the process of preparing Pickering W/O HIPEs and PDVB-SS-0.2-SO₃H is shown in Fig. 2. The internal (water) phase contained 80 mg of K₂SO₄, 40 mg of KPS and 200 mg of SS in 16.8 mL H₂O, and the external (oil) phase consisted of 3.0 mL of DVB, 40 mg of AIBN, 200 mg of hydrophobic silica nanoparticles, and 0.2 mL of span 80. When the internal and external phases were mixed, the phase-separated system was formed (Fig. 2a). Then, a stable Pickering W/O HIPE with an internal phase volume fraction of 84.8% was prepared after emulsification (Fig. 2b). Digital photographs of the drops of Pickering HIPEs dispersing in water and toluene are shown in Fig. 2c. The drops of the emulsions were diffused in toluene and maintained their original shape, indicating the formation of W/O Pickering HIPEs. In addition, the micrograph of the Pickering W/O HIPEs is shown in Fig. 2d, and the uniform and compact liquids revealed the typical type of HIPEs. The morphology of HIPEs was also observed by Xiaodong Li *et al.*²⁹ As shown in Fig. 2e, the digital photographs of PDVB-SS-0.2-SO₃H monolith soaking in water revealed that a lot of water permeated into the PDVB-SS-0.2-SO₃H monolith by pressing into the water *via* an external force. This indicates that a large number of interconnected pores exist inside the PDVB-SS-0.2-SO₃H monolith.

3.3 Characterizations of PDVB-SS-X-SO₃H

Fig. 3 shows the SEM images of PDVB-SS-0 (a), PDVB-SS-0-HF (b) (*i.e.* poly-Pickering-HIPEs removed silica nanoparticles by HF), the triangular domain of PDVB-SS-0-HF (c), PDVB-SS-0-HF-SO₃H (d), PDVB-SS-0.2-SO₃H (e), and PDVB-SS-0.6-SO₃H (f). Clearly, SEM image (Fig. 3a) shows that PDVB-SS-0 has a closed-cell pore structure (pore size of 100 ± 8 µm) but no pore throats are observed, indicating the impermeable nature of PDVB-SS-0. We learned preliminarily that the PDVB-SS-0 would exhibit the worst catalytic activity because the reactants and active sites of PDVB-SS-0-SO₃H may be isolated by closed-cell pores. An obvious double shell structure composed of poly-SS (PSS) internal layer and PDVB external layer is shown in Fig. 2b, and the formative reason may be that the SS monomers in water phase were moved to the interface of oil–water through a phase inversion process and form a PSS layer when the polymerization of PDVB-SS-0 emulsion occurs. In addition, upon enlarging the image of the triangular domain of PDVB-SS-0-HF (Fig. 2c), many clear 100 nm pores, which were formed by corroding the stabilized silica nanoparticles in HF are seen on the surface. The fact that the stabilized silica particles distribute in the triangle region to strengthen the stability of HIPEs was confirmed. Moreover, Silverstein *et al.*³⁰ also obtained the same result by TEM. The double shell and small pores structures of

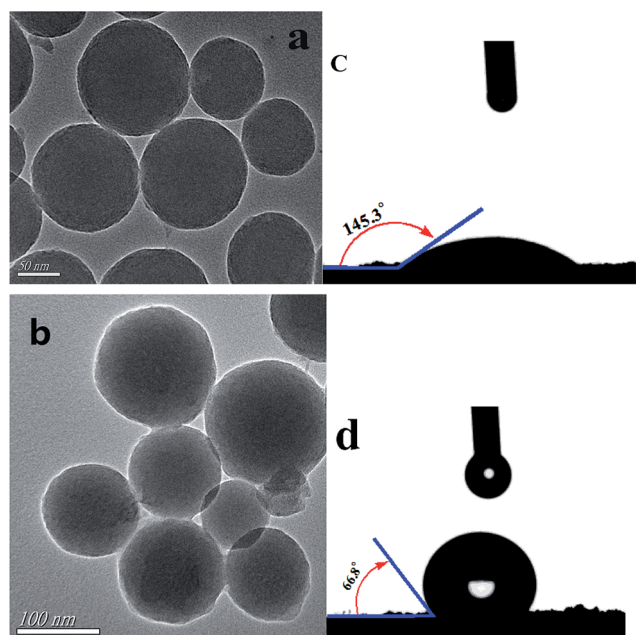


Fig. 1 TEM images of (a) silica nanoparticles, and (c) hydrophobic silica nanoparticles; contact angles of water images of (b) silica nanoparticles, and (d) hydrophobic silica nanoparticles.

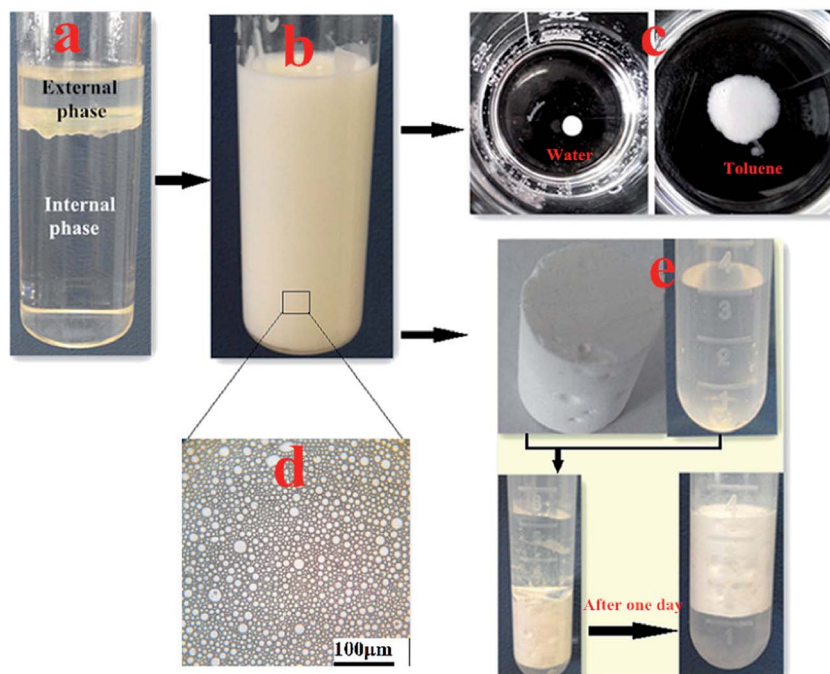


Fig. 2 Exposition of prepared Pickering W/O HIPEs and PDVB-SS-X-SO₃H using the experimental progress of PDVB-SS-0.2-SO₃H (a) phase-separated system, (b) Pickering W/O HIPEs with an 84.8 vol% internal phase fraction, (c) Pickering W/O HIPEs dispersed in water and toluene, (d) micrograph of the Pickering W/O HIPEs, (e) PDVB-SS-0.2-SO₃H monolith soaked in water.

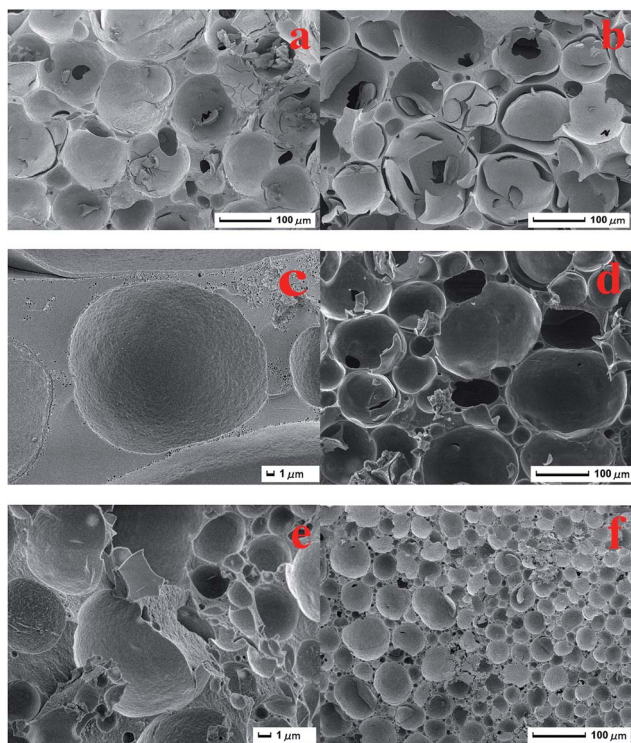


Fig. 3 SEM images of (a) PDVB-SS-0 (b) PDVB-SS-0-HF, (c) the triangular domain of PDVB-SS-0-HF, (d) PDVB-SS-0-HF-SO₃H, (e) PDVB-SS-0.2-SO₃H, and (f) PDVB-SS-0.6-SO₃H.

PDVB-SS-0-HF increased the odds of contact with reactants in the catalytic reaction. Meanwhile, we further sulfonated the PDVB-SS-0-HF, and discovered by SEM that the morphology

structure of PDVB-SS-0-HF-SO₃H (Fig. 3d) was similar to that of PDVB-SS-0-HF (Fig. 3b), which revealed that the sulfonation process had no obvious effect on material morphology. Moreover, this also suggested that PDVB-SS-X-SO₃H had excellent chemical and mechanical stability. With the increase in the volume of span 80, the different pore sizes of PDVB-SS-0-HF-SO₃H (Fig. 3d), PDVB-SS-0.2-SO₃H (Fig. 3e) and PDVB-SS-0.6-SO₃H (Fig. 3f) were obtained and were about 100 μm, 10 μm and 50 μm, respectively. The differences in the results of our observation may be attributed to three reasons, first, the adsorption of surfactant on particles promoted their attachment to the drop interface, leading to a decrease in the droplet size. Second, increasing the surfactant concentration lowered the oil-water interfacial tension, facilitating drop break up during emulsification.³¹ Thirdly, the droplets of W/O Pickering HIPEs are instability and easy to combined each other to form bigger droplets during polymerization process leading to form bigger pore sizes. Similar results have been also reported by Wong *et al.*³²

The results of energy dispersive spectrometer (EDS) analysis equipped with SEM for PDVB-SS-0, PDVB-SS-0-HF, PDVB-SS-0-SO₃H, PDVB-SS-0-HF-SO₃H, PDVB-SS-0.2-SO₃H, and PDVB-SS-0.6-SO₃H are listed in Fig. 4a–f, respectively. When comparing Fig. 4a and b, the peak of the element Si of PDVB-SS-0-HF disappeared, and the same phenomenon was observed in PDVB-SS-0-HF-SO₃H when comparing Fig. 4c and d, which suggested that the silica nanoparticles were successfully removed. Interestingly, as shown by Fig. 4a–d, the peaks of element S of PDVB-SS-0-SO₃H and PDVB-SS-0-HF-SO₃H were stronger than those of PDVB-SS-0 and PDVB-SS-0-HF, respectively, which indicated that the internal phase SS monomers were successfully

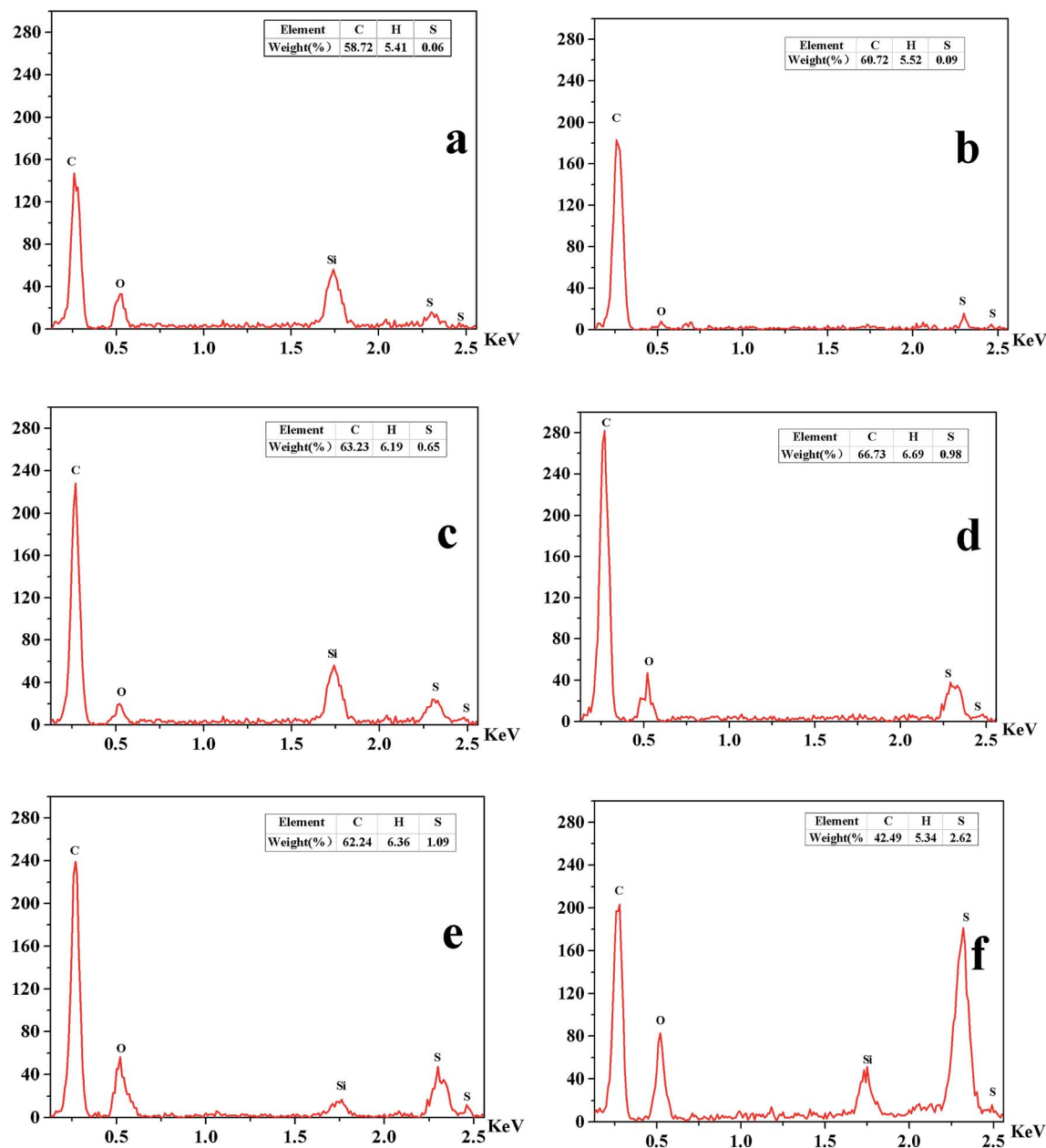


Fig. 4 Energy dispersive spectrometer (EDS) and elemental analysis of (a) PDVB-SS-0 (b) PDVB-SS-0-HF, (c) PDVB-SS-0-SO₃H, (d) PDVB-SS-0-HF-SO₃H, (e) PDVB-SS-0.2-SO₃H, and (f) PDVB-SS-0.6-SO₃H.

polymerized into PSS, and -SO₃H group was also grafted on PDVB *via* the sulfonation process. In addition, this fact could be further confirmed by SEM results of the formation of PSS layer. The peaks of elements S and O from PDVB-SS-0.6-SO₃H (Fig. 4f) were both evidently stronger than those of PDVB-SS-0.2-SO₃H (Fig. 4e). This result can be attributed to the formation of larger cell structure by Pickering HIEPs templates in the presence of more span 80, and that the larger pore was easier to be grafted by -SO₃H groups. The results of element analysis for PDVB-SS-0, PDVB-SS-0-HF, PDVB-SS-0-SO₃H, PDVB-SS-0-HF-SO₃H, PDVB-SS-0.2-SO₃H, and PDVB-SS-0.6-SO₃H are also shown in the corresponding figures. The weights of S in PDVB-SS-0-SO₃H (0.65%), PDVB-SS-0-HF-SO₃H (0.98%) and PDVB-SS-0.6-SO₃H

(2.62%) were increased than those of PDVB-SS-0 (0.06%), PDVB-SS-0-HF (0.09%) and PDVB-SS-0.2-SO₃H (1.09%), respectively, because -SO₃H groups were successfully grafted onto PDVB-SS-X-SO₃H. This was also confirmed by the results of the EDS analysis.

Fig. 5 shows the FT-IR spectra of PDVB-SS-0-HF-SO₃H (a) and PDVB-SS-0-SO₃H (b). The peaks of 1039 cm⁻¹, 1170 cm⁻¹ and 1487 cm⁻¹, which are associated with the C-S bond, -SO₃H group and benzene ring, respectively, could be clearly found in the samples of PDVB-SS-0-HF-SO₃H and PDVB-SS-0-SO₃H, suggesting the presence of sulfonic group and benzene ring in these samples.³³ The band around 1107 cm⁻¹ associated with Si-O-Si antisymmetric stretching vibration was only found in

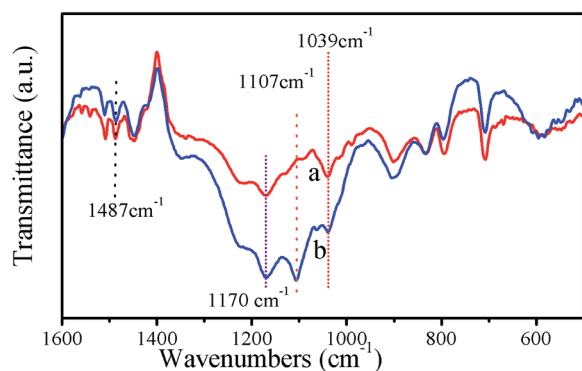


Fig. 5 FT-IR spectra of (a) PDVB-SS-0-HF-SO₃H, and (b) PDVB-SS-0-SO₃H.

the sample of PDVB-SS-0-SO₃H, suggesting that the silica nanoparticles were completely washed out by HF in the samples of PDVB-SS-0-HF-SO₃H. This result was also confirmed by the results of element and EDS analysis.

Fig. 6 shows the results of the X-ray photoelectron spectroscopy (XPS) measurements of PDVB-SS-0-HF-SO₃H and PDVB-SS-0-SO₃H. PDVB-SS-0-HF-SO₃H and PDVB-SS-0-SO₃H exhibited the signals of S, C and O, possibly indicating the presence of -SO₃H group in these samples. Correspondingly, the high resolution XPS spectrum of C1s showed that the signals at around 284.7 and 275.4 eV, associated with C-C and C-S bonds, respectively, could be found in these samples, further suggesting the successfully introduction of -SO₃H into

the network of PDVB-SS-X-SO₃H and that the -SO₃H group played a key role in increasing the acid strength of PDVB-SS-X-SO₃H. The signal of S2p of PDVB-SS-0-HF-SO₃H and PDVB-SS-0-SO₃H were found in the same position with a binding energy of 169 eV, suggesting no obvious effect of sulfonation for PDVB-SS-X-SO₃H after removing silica nanoparticles by HF. The results also supported the fact that PDVB-SS-X-SO₃H possessed rigid network structure and good chemical stability, which were also proven based on the morphology structure analysis of PDVB-SS-0-HF and PDVB-SS-0-HF-SO₃H performed earlier.

The acidic features of PDVB-SS-0-SO₃H, PDVB-SS-0-HF-SO₃H, PDVB-SS-0.2-SO₃H, and PDVB-SS-0.6-SO₃H solid catalysts were determined by NH₃-TPD. The physically adsorbed and hydrogen-bounded NH₃ can desorb at ≤150 °C,³⁴ and the acid site bound resulted in other desorbed NH₃ at higher temperatures.³⁵ In addition, the desorbed NH₃ at desorption temperatures of 150–250 °C, 250–350 °C, 350–500 °C and >500 °C were measured as weak, medium, strong and very strong of the acid sites, respectively.³⁶ As shown in Fig. 7, it can be clearly seen that medium, strong and very strong acid sites exist in PDVB-SS-X-SO₃H, and the areas of the peaks represented the amount of acidic sites, which are calculated and summarized in Table 2. The total acidic amounts of PDVB-SS-0-SO₃H, PDVB-SS-0-HF-SO₃H, PDVB-SS-0.2-SO₃H, and PDVB-SS-0.6-SO₃H were 170 μmol g⁻¹ (*i.e.* respective acidic amounts of 25 μmol g⁻¹, 69 μmol g⁻¹, and 76 μmol g⁻¹ for the acidic strengths of 300 °C, 470 °C and 578 °C), 207 μmol g⁻¹ (*i.e.* respective acidic amounts of 48 μmol g⁻¹, 76 μmol g⁻¹, and 83 μmol g⁻¹ for the acidic strengths of 289 °C, 420 °C and 578 °C), 233 μmol g⁻¹ (*i.e.*

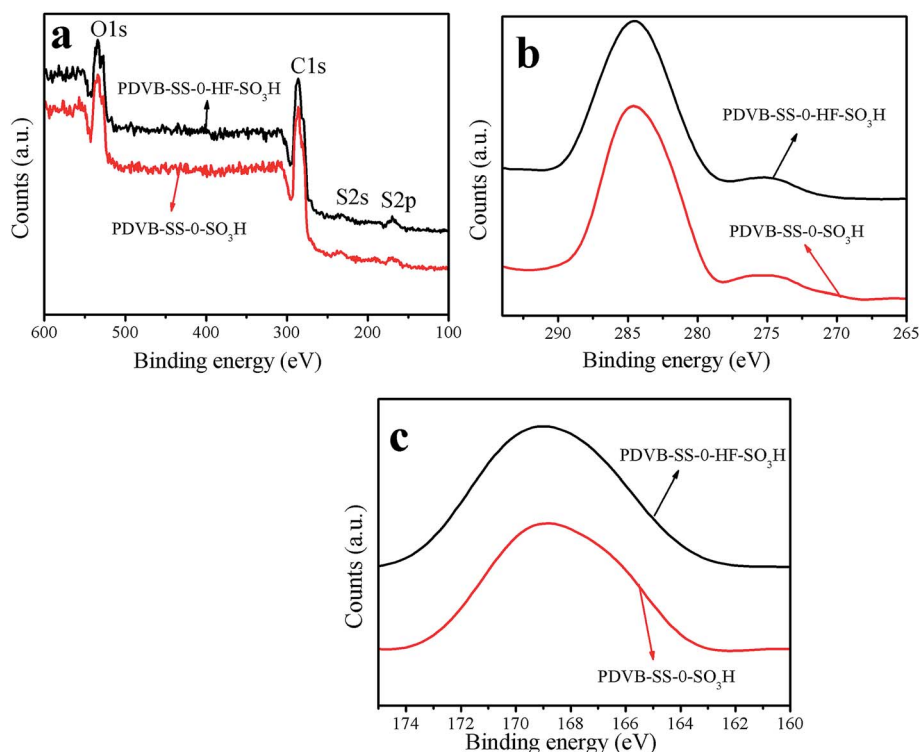


Fig. 6 X-ray photoelectron spectroscopy measurements of (a) survey, (b) C1s, (c) S2p of PDVB-SS-0-HF-SO₃H and PDVB-SS-0-SO₃H.

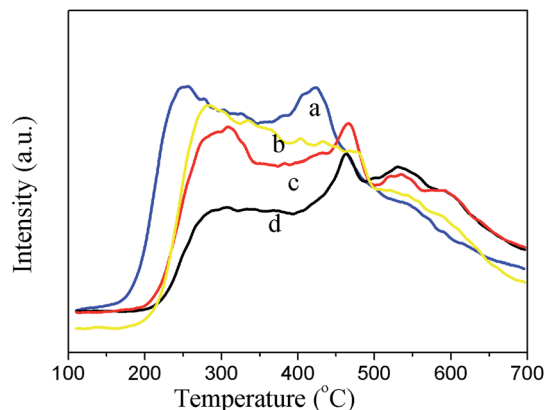


Fig. 7 NH_3 -TPD curves of (a) PDVB-SS-0.2- SO_3H , (b) PDVB-SS-0.6- SO_3H , (c) PDVB-SS-0-HF- SO_3H , and (d) PDVB-SS-0- SO_3H .

Table 2 Properties of the catalyst and catalytic efficiency

Sample ^a	Acid strength (°C)	Acid amounts ($\mu\text{mol g}^{-1}$)	Total acid amounts ($\mu\text{mol g}^{-1}$)	HMF (%)
PDVB-SS-0- SO_3H	300	25	170	12.9
	470	69		
	578	76		
PDVB-SS-0-HF- SO_3H	289	48	207	20.6
	420	76		
	578	83		
PDVB-SS-0.2- SO_3H	275	46	233	29.6
	379	92		
	548	95		
PDVB-SS-0.6- SO_3H	284	34	244	15.5
	359	69		
	508	141		

^a PDVB-SS-X- SO_3H , X stand for the volume of span 80.

respective acidic amounts of $46 \mu\text{mol g}^{-1}$, $92 \mu\text{mol g}^{-1}$, and $95 \mu\text{mol g}^{-1}$ for the acidic strengths of 275°C , 379°C and 548°C , and $244 \mu\text{mol g}^{-1}$ (*i.e.* respective acidic amounts of $34 \mu\text{mol g}^{-1}$, $69 \mu\text{mol g}^{-1}$, and $141 \mu\text{mol g}^{-1}$ for the acidic strengths of 284°C , 359°C and 508°C), respectively, which is in agreement with the results of the content of S of 0.65%, 0.98%, 1.09%, and 2.62% by elemental analysis, respectively. The acidic amount provides the number of acidic sites which can help in improving the efficiency of the conversion of cellulose to HMF.³⁷ In brief, PDVB-S S-X- SO_3H had much stronger acidic sites and the existence of this feature, *i.e.* $145 \mu\text{mol g}^{-1}$ at 470°C and 578°C for PDVB-SS-0- SO_3H , $159 \mu\text{mol g}^{-1}$ at 420°C and 578°C for PDVB-SS-0-HF- SO_3H , $187 \mu\text{mol g}^{-1}$ at 379°C and 548°C for PDVB-SS-0.2- SO_3H , and $210 \mu\text{mol g}^{-1}$ at 359°C and 508°C for PDVB-SS-0.6- SO_3H , could be effective to catalyze the reaction of cellulose to HMF.

3.4 Conversion of cellulose to HMF using PDVB-SS-X- SO_3H as the catalyst

The optimal reaction conditions for the conversion of cellulose to HMF using PDVB-SS-0.2- SO_3H as the catalyst were

determined by experience; the specific optimization reaction progress is listed as follows: first, cellulose (100 mg) was pre-treated in [Emim]Cl (2.0 g) at 120°C for 0.5 h. Then, the catalyst (40 mg) was added into the reactor and kept for another 3.0 h in the same condition. The effect of the different quantities of catalyst for the yield of HMF from cellulose under the same condition was studied, and the results are shown in Fig. 8a. It could be observed that only 9.8% yield of HMF was obtained when 20 mg of PDVB-SS-0.2- SO_3H was used at 120°C for 2.0 h but the yield of HMF unexpectedly reached to 29.6% as the amount of PDVB-SS-0.2- SO_3H increased to 40 mg, and the amount of catalyst was significantly lower than that of Wang Pan.³⁸ This fact indicated that the addition of PDVB-SS-0.2- SO_3H showed excellent catalytic performance in degrading cellulose to HMF. It may be because the increasing catalytic sites with the increased amount of catalyst boosts the dehydration reaction. However, when the amount of catalyst was increased from 40 mg to 60 mg, there was a smooth decrease in HMF yield. The same tendency of the HMF yield with the increasing amount of catalyst was also reported by Hu and co-workers.³⁹ This phenomenon implied that the side reaction of cellulose-degradation also accelerated due to the over-use of catalyst, which probably facilitated the decomposition of HMF or the polymerization of HMF.⁴⁰ Moreover, the addition of excess catalyst limited the mass transfer and decreased the amount of cellulose to join in the reaction at the same time.⁴¹

Meanwhile, we also studied the effects of reaction temperature and time on the yield of HMF from cellulose, and the results are shown in Fig. 8b. Under the same reaction time (*i.e.* 2.0 h and 40 mg of catalyst), 29.6% HMF yield at 120°C was significantly higher than the 15.3% HMF yield at 110°C , 21.6% HMF yield at 130°C , and 25.7% HMF yield at 140°C . This indicated that reaction temperature has a significant influence on the HMF yield. Proper high reaction temperature can accelerate the degradation of cellulose, and the decreasing trend was more obvious with higher reaction temperature, which suggested that higher reaction temperature can improve the rehydration and polycondensation of HMF to undesired byproducts such as soluble polymers and insoluble humins. Moreover, the same results were also obtained by Zhou and co-workers.⁴² There are two possible reasons. First, increasing the reaction temperature reduces the viscosity of ionic liquids and increases the contact area between the catalyst and the reactants, which was beneficial for the accelerated degradation of cellulose. Second, the by-product of HMF covered the acidic sites of catalysts, and the reaction of HMF to other substances was enhanced with the further increase in reaction temperature. Furthermore, the by-products, including formic acid and levulinic acid, were examined by HPLC; Zakrzewska and co-workers also reported that HMF was decomposed to some unidentified products.⁴³

To discuss the possible influence to the conversation of cellulose to HMF, the HMF yield of PDVB-SS-0- SO_3H (12.9%), PDVB-SS-0-HF- SO_3H (20.6%), PDVB-SS-0.2- SO_3H (29.6%) and PDVB-SS-0.6- SO_3H (15.5%) under the same conditions (40 mg of catalyst, 2.0 h of reaction time, and 120°C of reaction temperature) were obtained and are listed in Table 2. It is clear that

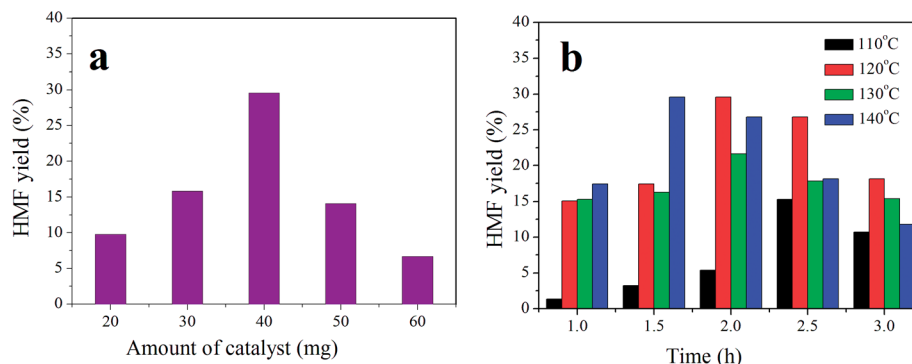


Fig. 8 Optimization of reaction conditions to cellulose to HMF using PDVB-SS-0.2-SO₃H as the catalyst. Effects of (a) the amount of PDVB-SS-0.2-SO₃H, and (b) reaction time and temperature under 40 mg of catalyst and 2.0 g of [Emim]Cl.

PDVB-SS-0.2-SO₃H obtained higher HMF yield. Moreover, according to the performance of PDVB-SS-X-SO₃H in the above-mentioned discussion, we observed that PDVB-SS-0.2-SO₃H had smaller pore sizes (about 10 μm) and moderate amount of strong acid (187 μmol g⁻¹). Thus, we concluded that the results may be attributed to two aspects: first, the smaller pore sizes helped in increasing contact frequency between reaction substrates and catalytic acid sites. Second, moderate amounts of strong acid was more conducive for the improvement of the catalytic effect.

3.5 Recycling of catalysis system

The recyclability of the catalyst is very important for the practical production of HMF and for the demand of green and sustainable chemistry. Therefore, the recycling activity of the catalyst was examined using a set of experiments. The solid acid catalyst PDVB-SS-0.2-SO₃H was recovered by filtering the mixture after the end of the first reaction, washing 10 times with 5.0 mL deionized water, and drying at 30 °C for 24 h in a vacuum oven. Subsequently, the solid acid catalysts were re-used for the conversion of cellulose to HMF up to four times under the same conditions, and the yields of HMF were 23.4%, 22.6%, 21.4%, and 20.3%. The loss of -SO₃H and the deposition of humins on the surface of the solid acid catalysts can lead to a decrease in HMF yield but the catalyst still retains good activity after re-using four times. Thus, the system of PDVB-SS-X-SO₃H can be effectively re-used.

4 Conclusion

In this work, PDVB-SS-X-SO₃H with adjustable porous structure were successfully synthesized by applying Pickering HPIEs template, and were used as solid super-acid catalysts to produce HMF from cellulose in a ionic liquid system. The porous properties and acidic features of the PDVB-SS-X-SO₃H were characterized, and the amount of catalyst (40 mg), reaction time (2.0 h), and reaction temperature (120 °C) were optimized for cellulose conversion in the presence of PDVB-SS-0.2-SO₃H. 29.6% yield of HMF was obtained in the PDVB-SS-0.2-SO₃H catalyzed system, which was superior to the

PDVB-SS-0.6-SO₃H system with 15.5%, PDVB-SS-0-HF-SO₃H system with 20.6%, and PDVB-SS-0-SO₃H system with 12.9%. It could be concluded that the pore sizes and acidic features of PDVB-SS-X-SO₃H were important for the conversion of cellulose to HMF. This work is being continued in an effort to prepare macroporous polymerized solid acids, and the results of this work have provided useful experience for future research toward the development of new energy, especially in the area of bioenergy.

Acknowledgements

This work was financially supported by the National Natural Science Foundation of China (no. 21107037, no. 21176107, no. 21306013), Natural Science Foundation of Jiangsu Province (no. BK20131223), National Postdoctoral Science Foundation (no. 2013M530240), Special National Postdoctoral Science Foundation (no. 2014T70480), Postdoctoral Science Foundation funded Project of Jiangsu Province (no. 1202002B) and Programs of Senior Talent Foundation of Jiangsu University (no. 12JDG090).

References

- 1 D. M. Alonso, J. Q. Bond and J. A. Dumesic, *Green Chem.*, 2010, **12**, 1493–1513.
- 2 L. Hu, G. Zhao, W. W. Hao, X. Tang, Y. Sun, L. Lin and S. J. Liu, *RSC Adv.*, 2012, **2**, 11184–11206.
- 3 L. Y. Roman, C. J. Barrett and Z. Y. Liu, *Nature*, 2007, **447**, 982–985.
- 4 M. Balakrishnan, E. R. Sacia and A. T. Bell, *Green Chem.*, 2012, **49**, 1626–1634.
- 5 K. M. Rapp, US 4740605, 26-04-1988.
- 6 F. S. Asghari and H. Yoshida, *Ind. Eng. Chem. Res.*, 2006, **45**, 2163–2173.
- 7 I. Jiménez-Morales, J. santamaria-González, P. Maireles-Torres and A. Jiménez-López, *Appl. Catal., B*, 2011, **103**, 91–98.
- 8 L. A. S. do Nascimento, L. M. Z. Tito, T. S. Angelica, C. E. F. da Costa, J. R. Zamian and G. N. da Rocha Filho, *Appl. Catal., B*, 2011, **101**, 495–503.

- 9 B. V. S. K. Rao, K. C. Mouli, N. Rambabu, A. K. Dalai and R. B. N. Prasad, *Catal. Commun.*, 2011, **14**, 20–26.
- 10 M. Toda, A. Takagaki, M. Okamura, J. N. Kondo, K. Domen, S. Hayashi and M. Hara, *Nature*, 2005, **438**, 178.
- 11 G. Pasquale, P. Vázquez, G. Romanelli and G. Baronetti, *Catal. Commun.*, 2012, **18**, 115–120.
- 12 C. Tagusagawa, A. Takagaki, K. Takanabe, K. Ebitani, S. Hayashi and K. Domen, *J. Catal.*, 2010, **270**, 206–212.
- 13 Z. H. Zhang, K. Dong and Z. K. Zhao, *ChemSusChem*, 2011, **4**, 112–118.
- 14 L. Hu, G. Zhao, X. Tang, Z. Wu, J. X. Xu, L. Lin and S. J. Liu, *Bioresour. Technol.*, 2013, **148**, 501–507.
- 15 J. Liu, W. P. Kong, C. Qi, L. F. Zhu and F. S. Xiao, *ACS Catal.*, 2012, **2**, 565–572.
- 16 F. Liu, *Appl. Catal., B*, 2013, **136**, 193–201.
- 17 C. Tagusagawa, A. Takagaki, A. Iguchi, K. Takanabe, J. N. Kondo, K. Ebitani, T. Tatsumi and K. Domen, *Chem. Mater.*, 2010, **22**, 3072–3078.
- 18 Y. L. Zhang, J. M. Pan, Y. S. Yan, W. D. Shi and L. B. Yu, *RSC Adv.*, 2014, **4**, 23797–23806.
- 19 Y. L. Zhang, J. M. Pan, Y. S. Yan, W. D. Shi and L. B. Yu, *RSC Adv.*, 2013, **4**, 11664–11672.
- 20 Y. Yu, J. W. Zeng, Y. W. Chao and T. Zhen, *Chem. Commun.*, 2013, **49**, 7144–7146.
- 21 N. R. Cameron, *Polymer*, 2005, **46**, 1439–1449.
- 22 S. D. Kimmins and N. R. Cameron, *Adv. Funct. Mater.*, 2011, **21**, 211–225.
- 23 A. Menner, R. Powell and A. Bismarck, *Macromolecules*, 2006, **39**, 2034–2035.
- 24 V. O. Ikem, A. Menner and A. Bismarck, *Angew. Chem., Int. Ed.*, 2008, **47**, 8277–8279.
- 25 V. O. Ikem, A. Menner, T. S. Horozov and A. Bismarck, *Adv. Mater.*, 2010, **22**, 3588–3592.
- 26 W. Stöber, A. Fink and E. Bohn, *J. Colloid Interface Sci.*, 1968, **26**, 62–69.
- 27 H. H. Wei, Y. L. Yin, H. P. Wun and C. W. W. Kevin, *Catal. Today*, 2011, **174**, 65–69.
- 28 B. P. Binks and S. Lumsdon, *Phys. Chem. Chem. Phys.*, 2000, **2**, 2959–2967.
- 29 X. D. Li, G. Q. Sun, Y. C. Li, J. C. Yu, J. Wu, G. H. Ma and T. Ngai, *Langmuir*, 2014, **30**, 2676–2683.
- 30 I. Gurevitch and M. S. Silverstein, *Macromolecules*, 2011, **44**, 3398–3409.
- 31 S. W. Zou, Y. Yang, H. Liu and C. Y. Wang, *Colloids Surf., A*, 2013, **436**, 1–9.
- 32 L. L. C. Wong, V. O. Ikem, A. Menner and A. Bismarck, *Macromol. Rapid Commun.*, 2011, **32**, 1563–1568.
- 33 J. Scaranto, A. P. Charmet and S. Giorgianni, *J. Phys. Chem. C*, 2008, **112**, 9443–9447.
- 34 D. Liu, P. Yuan, H. M. Liu, J. G. Cai, Z. H. Qin, D. Y. Tan, Q. Zhou, H. P. He and J. X. Zhu, *Appl. Clay Sci.*, 2011, **52**, 358–363.
- 35 R. C. Ravindra, Y. S. Bhat, G. Nagendrappa and B. S. Jai Prakash, *Catal. Today*, 2009, **141**, 157–160.
- 36 D. Liu, P. Yuan, H. M. Liu, J. G. Cai, D. Y. Tan, H. P. He, J. X. Zhu and T. H. Chen, *Appl. Clay Sci.*, 2013, **80**, 407–412.
- 37 P. Kalita, B. Sathyaseelan, A. Mano, S. M. Javaid Zaidi, M. A. Chari and A. Vinu, *Chem.–Eur. J.*, 2010, **16**, 2843–2846.
- 38 P. Wang, H. B. Yu and S. H. Zhan, *Bioresour. Technol.*, 2011, **102**, 4179–4183.
- 39 L. Hu, G. Zhao, X. Tang, Z. Wu, J. X. Xu, L. Lin and S. J. Liu, *Bioresour. Technol.*, 2013, **148**, 501–507.
- 40 Q. Zhao, L. Wang, S. Zhao, X. H. Wang and S. T. Wang, *Fuel*, 2011, **90**, 2289–2293.
- 41 C. Aellig and I. Hermans, *ChemSusChem*, 2012, **5**, 1737–1742.
- 42 L. L. Zhou, R. J. Liang, Z. W. Ma, T. H. Wu and Y. Wu, *Bioresour. Technol.*, 2013, **129**, 450–455.
- 43 M. E. Zakrzewska, E. Bogel-Lukasik and R. Bogel-Lukasik, *Chem. Rev.*, 2011, **111**, 397–417.